Effect of piperine coated gold nanoparticles on amyloid fibril formation of insulin

Insulin fibril assembly is known to be directly linked to type II diabetes (Luo et al. 2016). Aggregation of normal functional proteins such as insulin into amyloid fibrils has also been reported to be linked to many medical severities (Chatani et al. 2014)(Wei et al. 2009)(F. Wang et al. 2001). The storage of insulin as therapeutic agent is also a big concern because of the tendency of insulin molecules to form amyloid aggregates (Liza Nielsen et al. 2001)(Brange et al. 1992). Formation of amyloid like aggregates of insulin has been reported in the artery walls located at the site of injection (F. Wang et al. 2001). Hence, one of the effective strategies to target that aggregation linked severities could be the prevention of the process of protein aggregation.

In this chapter, to target protein aggregation, uniform sized (~10 nm) gold nanoparticles which are surface functionalized with piperine were synthesized and their inhibition effect on amyloid fibril formation of insulin under *in vitro* conditions has been tested. The inhibition effect of piperine coated gold nanoparticles on both spontaneous and seed-induced aggregation of insulin has been examined. Using both experimental and computational approach the possible molecular interaction between piperine and insulin was also analyzed. Finally, the hemocompatibility of piperine coated nanoparticles has been also tested.

5.1 EFFECT OF PIPERINE COATED NANOPARTICLES ON INSULIN FIBRIL ASSEMBLY.

Successful designing of effective inhibitors of protein aggregation process has gained much attention in recent years. Several candidates including single molecules, amino acids, natural compounds, peptides and proteins have been reported to act as inhibitors of amyloid fibril formation of different proteins (Ghosh et al. 2009)(Kar and Kishore n.d.)(Shiraki et al. 2002)(Rajasekhar et al. 2015)(Viet et al. 2011). Over the past decade much research has also focused on the surface functionalization of metallic nanoparticles with potential compounds to target amyloid formation of proteins (Dubey et al. 2015) (Álvarez et al. 2013) (Siposova et al. 2012)(Palmal, Maity, et al. 2014a). Various properties of the nanoparticles, such as their size and thermal stability, are critical factors for their inhibition effect against amyloid fibril formation of proteins. Some studies have also reported that the anti-amyloid activity of inhibitors is greatly enhanced when these inhibitor molecules are surface functionalized with the nanoparticles (Dubey et al. 2015)(Anand et al. 2016b).

In the current chapter, the antiamyloid effect of piperine coated old nanoparticle has been tested against fibril assembly of insulin under *in vitro* conditions. Molecular docking studies and quenching studies have been performed to understand the role of surface functionalization and the role of protein-ligand interaction during inhibition of protein aggregation. Finally, the hemocompatiblity of the prepared piperine coated gold nanoparticles has also been examined by following in vitro hemolysis assay tools. Studies have also been performed to check the inhibition effect of piperine coated gold nanoparticles on fibril assembly process of serum albumin and collagen proteins.

5.1.1 Selection of piperine to target insulin fibril assembly.

Piperine is a natural compound known for its multiple health benefits and some of its medical benefits are listed in Table 5.1. The piperine molecule has a unique structure (Figure 5.1a), which is known to interact with proteins and DNA through viable H-bonds mediated through its C=O and –O– functional groups (Chinta et al. 2015)(Zsila et al. 2005)(Haris et al. 2015)(Yeggoni et al. 2015). Formation of strong H-bonds between piperine and valine residues of protein molecules has already been reported.

Table 5.1: Reports on multiple medical benefits of piperine

Molecule	Applications
Piperine	Increase the absorption of selenium, vitamin B and β- carotene as well as other nutrients(Rajinder K Bhardwaj et al. 2002)
	Stimulate pancreatic and intestinal digestive enzymes and increases biliary bile acid secretion(Tiwari et al. 2008)
	Prevents and minimizes diarrhea produced by various oil(Reshmi et al. 2010)
	Anti-inflammatory, thermogenic, growth stimulatory, anti-thyroid and chemo preventive activities(Panda 2003)
	Antipyretic, analgesic, insecticidal, immunomodulatory, antitumor, anti-depressant and anti-apoptotic activities (Sunila and Kuttan 2004)(S. Li et al. 2007)
	Inhibition of hepatic drug metabolism (Ganesh Bhat and Chandrasekhara 1987)
	Enhancing pentobarbitone induced hypnosis (Mujumdar et al. 1990)
	Enhancing hepatoprotective activity (Desaiet al. 2008)
	Inhibition of lipid peroxidation during experimental inflammation(Dhuley et al. 1993)
	Antifertility(Daware et al. 2000)
	Radio protective effects(D'Hooge et al. 1996)
	Analgesic, anti-convulsant, anti-arthritic, anti-ulcer, antioxidant activities and cytoprotective effects(Kapoor et al. 2009)
	Bioavailability enhancer in the formulations of several drugs(Sharma et al. 2000)
	Inhibit human CYP3A4, P-glycoprotein, transport of xenobiotics and metabolites(R. K. Bhardwaj 2002)
	Stimulate pigmentation in the skin(Faas et al. 2008)

Studies have revealed that "LVEALYL" segment of the B-chain of insulin plays a key role to begin the fibril formation of the protein (Ivanova et al. 2009) (Ivanova et al. 2006). Peptides containing "LVEALYL" sequence have been reported to influence the aggregation properties of insulin. Based on these evidences, it was hypothesized that piperine could be an effective molecule to interact with "LVEALYL" segment of insulin's B chain, preferably with the valine residue. It was postulated that such piperine-insulin interaction would restrict the initiation of insulin fibril assembly. Since surface functionalization of inhibitor molecules on nanoparticles have been reported to greatly strengthen their inhibition efficacies against the process of protein aggregation(Dubey et al. 2015)(Anand et al. 2016b), this work has synthesized gold nanoparticles surface-functionalized with piperine, to target aggregation prone segment (LVEALYL) of insulin.

5.1.2 Synthesis and characterization of piperine coated gold nanoparticles.

Stable gold nanoparticles which are surface functionalized with piperine ($AuNPs^{piperine}$) were synthesized by following the established protocol(Dubey et al. 2015b) (see method section in Annexure A), as schematically represented in the panel a of Figure 1. The UV-Visible spectra of $AuNPs^{piperine}$ sample showed a distinct SPR peak at ~530 nm (Figure 5.1e). Dynamic light scattering data of $AuNPs^{piperine}$ sample clearly showed a homogeneous population of nanoparticles with average hydrodynamic radius of ~10 nm (Figure 5.1f). The value of the surface charge obtained for these $AuNPs^{piperine}$ was found to be -4.46 mV, as evident from the Zeta potential measurements (Figure 5.2). Transmission electron microscopy (TEM) images further confirmed the formation of homogenous species of spherical $AuNPs^{piperine}$ (Figure5.1b).

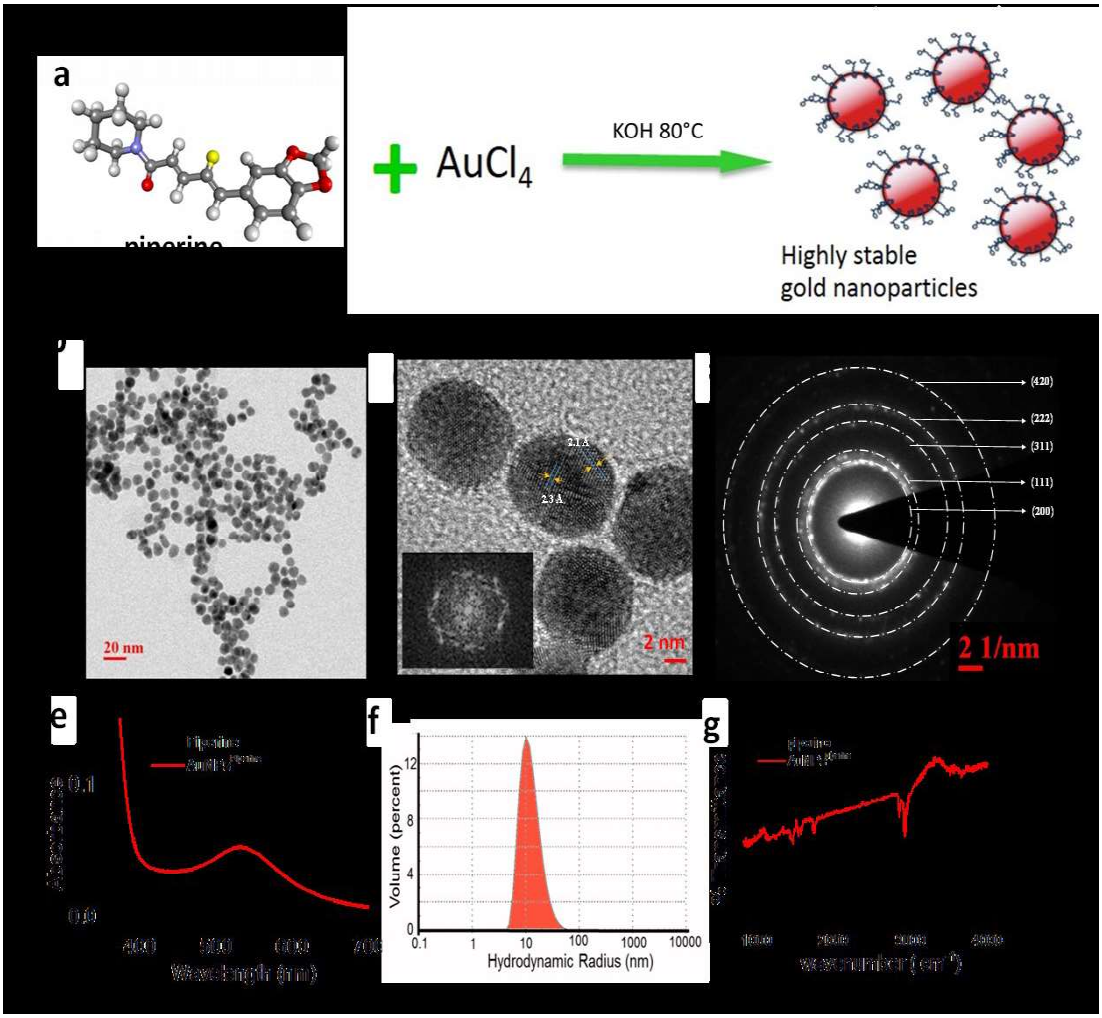

Figure 5.1: Thermal Characterization of piperine coated gold nanoparticles ($AuNPs^{piperine}$) **(a)** Schematic representation of the surface functionalized gold nanoparticles. **(b)** TEM images displaying the evenly sized (~10nm) spherical $AuNPs^{piperine}$ **(c)** HR TEM data showing a fringe spacing of 2.1 and 2.3Å. Inset shows splitting of spots in the FFT image. **(d)** The selected area electron diffraction pattern (SAED) of $AuNPs^{piperine}$. Scherrer ring patterns indicate the FCC gold is nanocrystalline in nature. **(e)** UV-Vis spectrum of $AuNPs^{piperine}$ with absorption maxima around 530 nm due to surface plasma resonance. **(f)** Dynamic Light Scattering (DLS) peak of $AuNPs^{piperine}$ showing an average diameter of ~10 to 20 nm. **(g)** FTIR Spectra of (—) piperine and (—) AuNPspiperine nanoparticles.

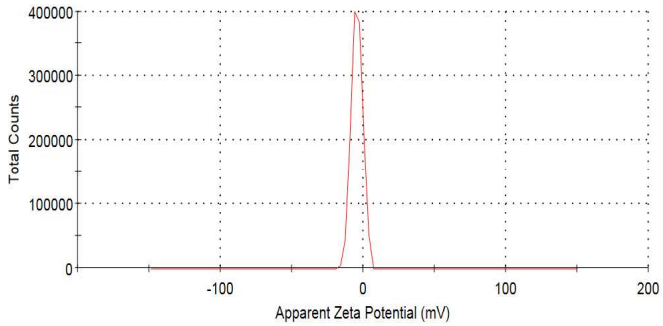

Figure 5.2. The surface zeta potential graph for piperine coated gold nanoparticles ($AuNPs^{piperine}$) showing a negative potential of -4.46 mV.

To understand the chemistry of surface functionalization of piperine molecules with the nanoparticles, ATR-FTIR measurements were conducted for both uncoated and coated piperine samples. Panel g of Figure 5.1 compares the FTIR signatures obtained for both control piperine (black curve) and surface-functionalized piperine ($AuNPs^{piperine}$) samples (red curve). The

piperine molecule consists of a piperidine moiety, a methylene dioxy phenyl ring or dioxol group and a CH stretch(Schulz and Baranska 2007). The FTIR-spectra of isolated piperine (black curve, Figure 5.1g) sample showed the presence of several characteristic peaks as reported earlier (Schulz and Baranska 2007). The FTIR spectra of AuNPs^{piperine} sample showed disappearance of the peaks region linked to = C – O group (red curve, Figure 5.1g). This result suggests that the gold nanoparticles may be surface-functionalized with the dioxol group. Further, we have characterized the thermal stability of AuNPs^{piperine} sample by exposing these samples to 70˚C, the temperature at which all the fibril assembly reactions were carried out. The SPR peaks of the samples remained unaltered even after several days of incubation at 70˚C (Figure 5.3). This signifies that these nanoparticles are very thermostable which may act as good candidates for preventing temperature induced insulin aggregation.

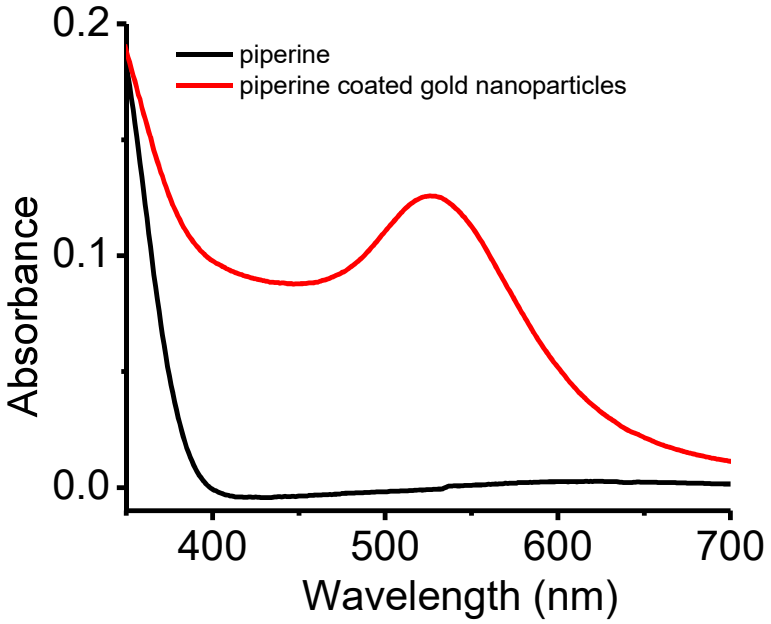

Figure 5.3. Stability of AuNPs^{piperine} UV-Vis spectrum of AuNPs^{piperine} with an absorption maximum around 530 nm due to surface plasma resonance. Red curve is AuNPs^{piperine} sample after 28 days; black curve is only piperine after 28 days. The solvent for both the samples was 1X PBS buffer at pH 7.4.

To further characterize the intrinsic structural properties of the AuNPs ^{piperine} nanoparticles, high-resolution TEM (HRTEM) was performed which confirmed the polycrystalline nature of the nanoparticles (Figure 5.1c). To throw light into the nature of alignment of crystalline fringes, the HRTEM image using FFT (Gatan digital micrograph software) were analyzed and the data displayed fringe patterns with d spacing of 2.1 Å (suggesting (111) FCC crystal) and 2.3Å (suggesting (200) index in FCC crystals) (inset of Figure 5.1c). The SAED (the selected area electron diffraction) pattern of these AuNPs^{piperine} nanoparticles using image J software were then examined and the ring patterns of the obtained data revealed (111), (222), (220), (311), and (420) indexed face-centered cubic crystal (fcc) structure for the nanoparticles (Figure 5.1d).

Control gold nanoparticles without piperine were generated using citrate mediated protocol (Gangwar et al. 2012). The SPR peak for these nanoparticles was observed at 535 nm (Figure 5.4) and the hydrodynamic radius of these particles was found to vary within 10-40 nm (Figure 5.4). The surface charge of these citrate capped gold nanoparticles was found to -19.5 mV (Figure 5.4). TEM images of these nanoparticles also revealed the presence of spherical nanoparticles of 10-20 nm of size (Figure 5.4).

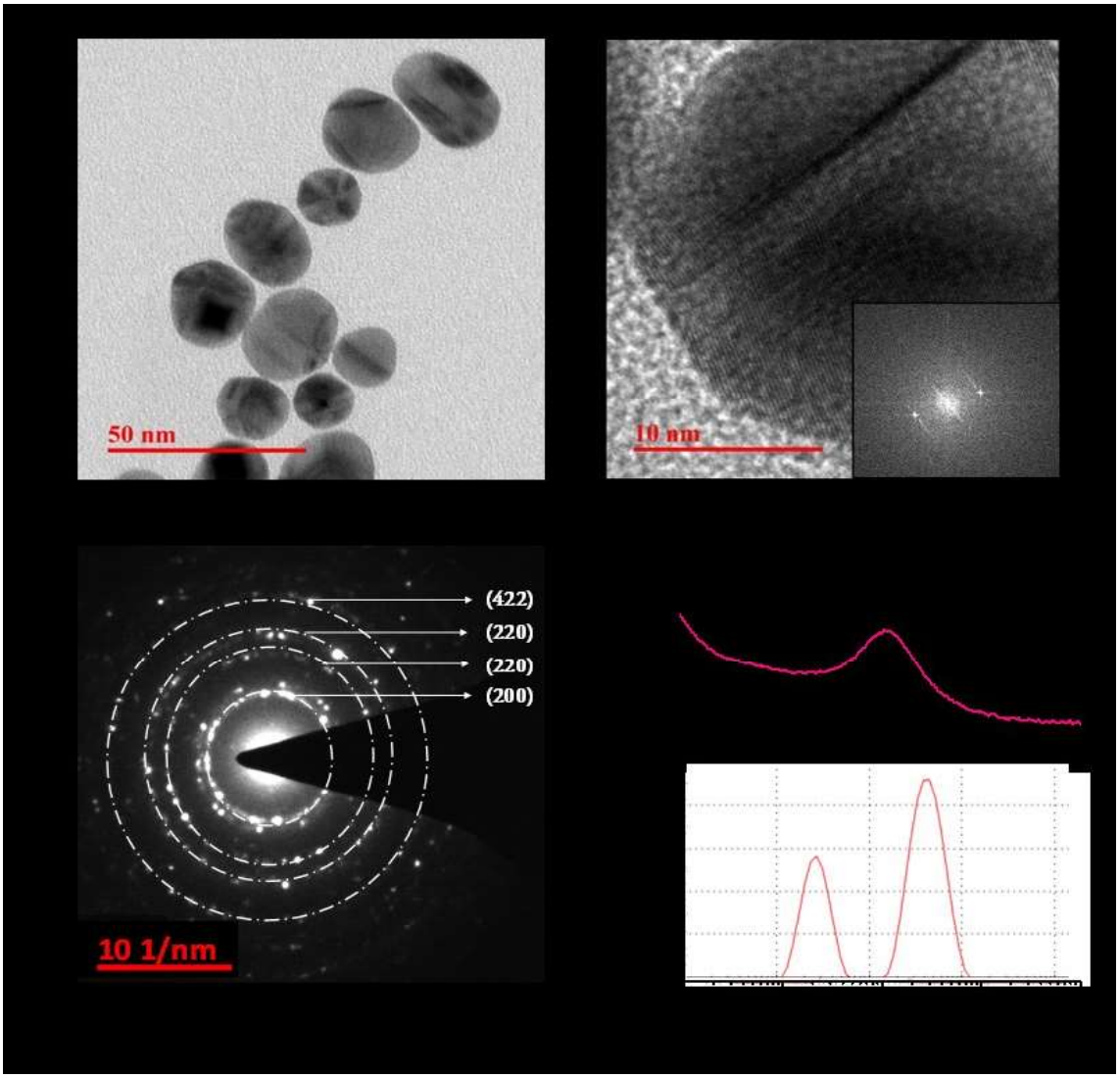

Figure 5.4. Characterization of control gold nanoparticles AuNPs without piperine. (a)TEM images displaying the evenly sized spherical AuNPs ranging from ~ 10-40nm (b) HR TEM reveal a fringe spacing of 2.1 Å and 2.3Å. Inset shows a selected area electron diffraction pattern (SEAD) of AuNPs samples. (c) The Scherrer ring patterns indicate the nanocrystalline nature of FCC gold. (d) UV-Vis spectrum of AuNPs with an absorption maximum (λ_{max}) of ~535 nm. (f) Dynamic Light Scattering (DLS) data indicate the average diameter of ~10 to 40 nm for AuNPs.

Crystallinity of the citrate capped gold nanoparticles showed fringe patterns of fringe with d spacing of 2.3Å, indicating (200) index in FCC crystal. The SAED analysis of the citrate capped gold nanoparticle revealed the existence of (111) and (420) planes with a *d*-spacing of 2.3 Å and 9.1Å respectively.

5.1.3. Effect of piperine coated nanoparticle on insulin fibril assembly: Amyloid fibril formation of insulin was initiated by incubating the protein monomers at 70°C in PBS at pH 7 (Dubey et al. 2015)(Dubey et al. 2014) and the aggregation reaction was monitored by reading the fluorescence signal of Thioflavin T, the amyloid specific dye (Lee et al. 2011b). Thioflavin T assay data, as shown in the panel *a* of Figure 5.5, display the effect of both piperine, $AuNPs^{piperine}$ on the process of insulin fibril assembly. Only insulin without any additives followed a typical aggregation kinetics pattern (Figure 5.5a, ■) as reported in previous studies(Dubey et al. 2015b). However, in the presence of $AuNPs^{piperine}$, strong inhibition of the

aggregation process was observed, in a dose dependent manner (Figure 5.5a, ◄, ►, ◆). Isolated piperine (Figure 2a, ▼, ●, ▲), at similar concentrations, showed slight inhibition of insulin aggregation, which suggests the significance of surface functionalization of nanoparticles with piperine. Also, no such inhibition effect was observed in the presence of control gold nanoparticles (data not shown). The fluorescence images of the Thioflavin T stained fibrils (Figure 5.5d) obtained from both inhibited and uninhibited aggregation reactions correlated well with the aggregation data (Figure 5.5a). Further testing was performed to understand the effect of these AuNPs^{piperine} on seed-induced fibril assembly of insulin. The results, as shown in Figure 5.5c, clearly showed suppression of seed-induced fibril formation of insulin in the presence of AuNPs^{piperine}.

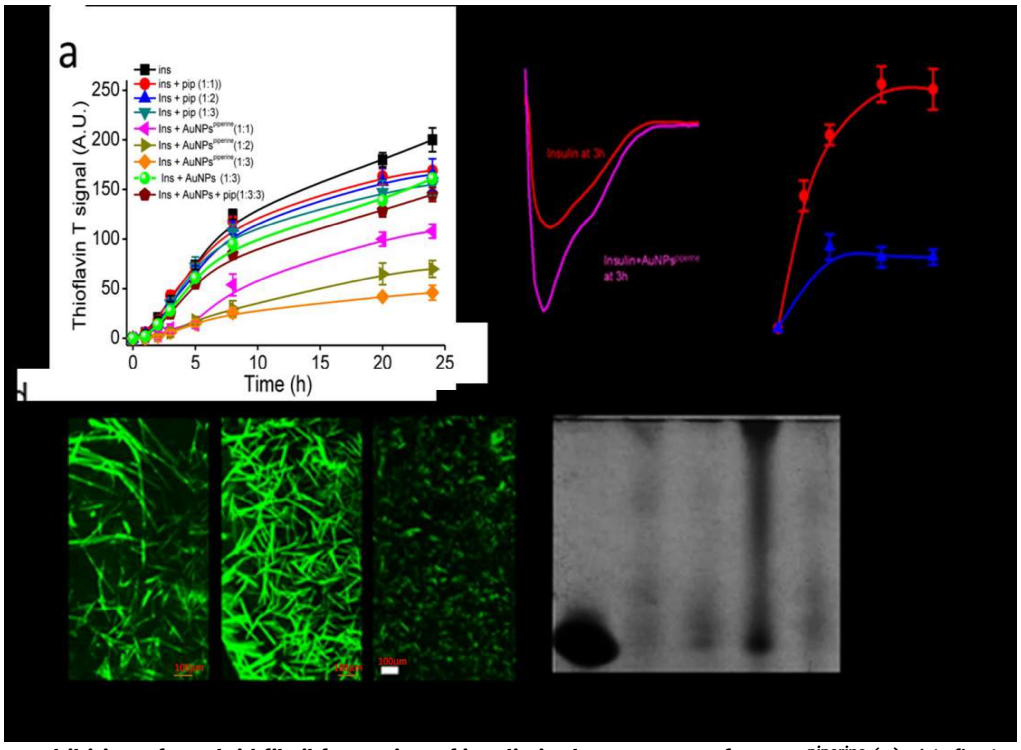

Figure 5.5 Inhibition of amyloid fibril formation of insulin in the presence of AuNPs^{piperine} (a) Thioflavin T assay data showing aggregation curves for 43 μM of insulin sample in PBS at pH 7: (■) insulin only; (●) insulin +piperine (1:1); (▲) insulin + piperine (1:2); (▼) insulin + piperine (1:3); (◄) insulin + AuNPs^{piperine} (1:1); (►) insulin + AuNPs^{piperine} (1:2); (◆) insulin + AuNPs^{piperine} (1:3). (b) CD spectra of insulin sample (43 μM) undergoing aggregation in the presence and in the absence of AuNPs^{piperine}: (black) insulin at 0 h; (red) insulin at 3 h; (blue) insulin + AuNPs^{piperine} (1:3 molar ratio) at 3 h. CD curve for inhibited reaction was obtained after baseline subtraction with the CD signal of AuNPs^{piperine} sample in PBS. (c) Inhibition of seed-induced aggregation of 43 μM insulin in the presence of AuNPs^{piperine} at 1:3 molar ration of protein: inhibitor. ~15% w/w preformed fibrils were used as seed. (d) Fluorescence images showing the presence of ThT stained fibrils, as labeled. (e) Native PAGE of insulin samples in the presence and in the absence of AuNPs^{piperine} during aggregation: (1) soluble insulin at 0h; (2) aggregating insulin sample at 3h, (3) aggregating [insulin+piperine] sample at 3h (4) aggregating [insulin+ AuNPs^{piperine}] sample at 3h (5) aggregating [insulin+ control AuNPs] sample at 3h. Molar ratio of protein to inhibitor was maintained at 1:3 for all Native PAGE experiments.

To see whether AuNPs^{piperine} can retain the native insulin structure during aggregation, native PAGE experiments were conducted on insulin samples undergoing fibril assembly. Panel e of Figure 5.5 shows the respective bands obtained for aggregating insulin samples in the presence and in the absence of inhibitors at 3 h time point. The results clearly indicate the retention of native structures of insulin in the presence of AuNPs^{piperine} (panel e, Figure 5.5b). To further confirm this result. The circular dichroism measurements on these samples (magenta curve, panel b, Figure 5.5) also confirmed the retention of native structures of insulin in the presence of AuNPs^{piperine}.

In the next step, the aggregation experiments were extended to another globular protein, bovine serum albumin (BSA), and the results obtained are summarized in the Figure 5.6. The data shown in Figure 5.6 indicated similar inhibition effect of AuNPs^{piperine} on amyloid fibril formation of serum albumin. Slightly higher molar ratio of protein: inhibitor was, however, was required to achieve the inhibition BSA aggregation.

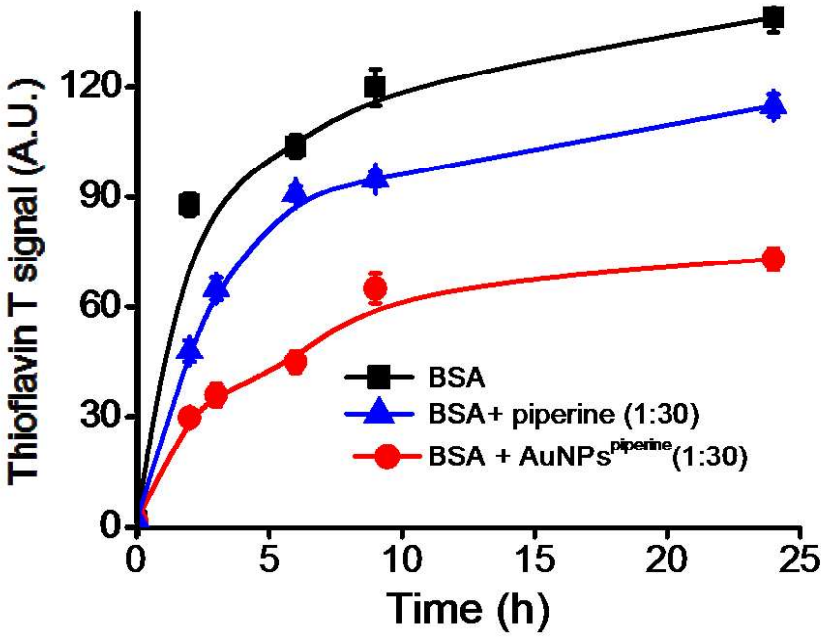

Figure 5.6. Inhibition of amyloid fibril formation of serum albumin in the presence of AuNPs^{piperine}**.** Thioflavin T assay data showing aggregation curves for ~5 μM of BSA sample in PBS at pH 7: (■) BSA only; (▲) BSA + piperine (1:30); (●) insulin + AuNPs^{piperine} (1:30).

5.1.4 Quenching studies on the interaction between insulin and AuNPs^{piperine}

It is has been reported that stabilization of the native protein structure is one of the critical factors to prevent the process of amyloid aggregation of proteins (Soldi et al. 2006). The results from CD and Native PAGE experiments also pointed to the retention of native insulin species in the presence of AuNPs^{piperine} (Figure 5.4b, 5.4e). Hence, to gain more insights into piperine-insulin interaction, both computational and fluorescence quenching experiments were conducted. First, the quenching effect of AuNPs^{piperine} on insulin native monomers was examined (see methods, Annexure A) and the data are shown in Figure 5.7a. The intensity of fluorescence emission of insulin was efficiently quenched in the presence of AuNPs^{piperine} in a dose dependent manner. Using the obtained quenching data, the Stern-Volmer constant (K_{sv}) (panel b, Figure 5.7) was calculated and the value was found to be ~4.48×10^4 M^{-1}. Further analysis of the obtained fluorescence quenching data was performed to predict the binding constant (K_a) and the binding site parameter (n) (see methods). Binding constant (K_a) parameter, obtained from the plot of $log\ (F_0\text{-}F)/F$ vs $log\ [Q]$(Yeggoni et al. 2015) was found to be 4.23 (±1.5) x 10^2 M^{-1}. The calculated binding site parameter (n) was found to be ~ 0.6, indicating a single binding site within the insulin molecule.

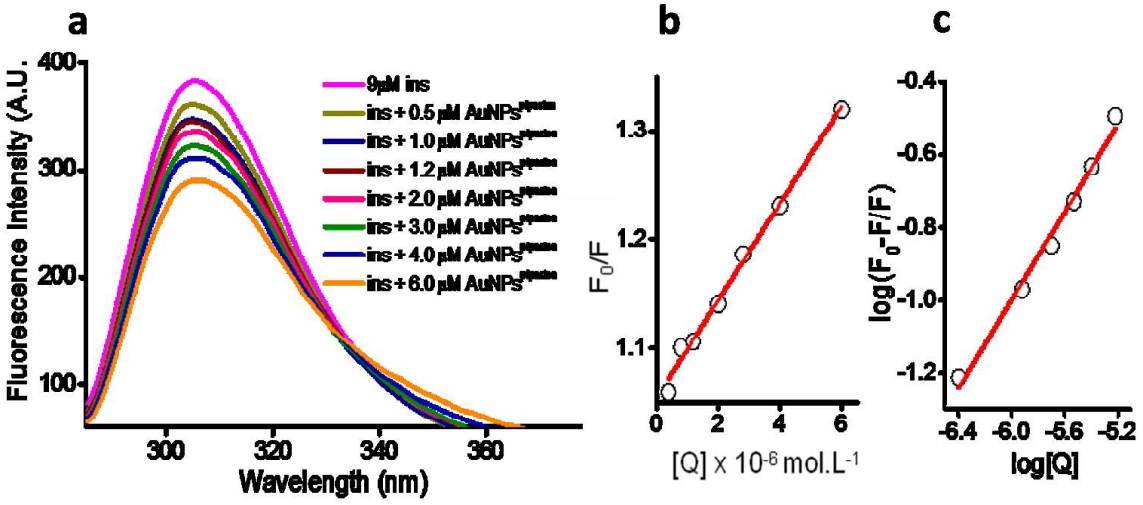

Figure 5.7. Interaction of piperine coated gold nanoparticles with insulin monomers. (a) Fluorescence emission spectra of 9 μM insulin sample with increasing concentration of $AuNPs^{piperine}$. Excitation wavelength was 276 nm. Concentrations of $AuNPs^{piperine}$ were: (—) 0 μM; (—) 0.5 μM; (—) 1 μM; (—) 1.2 μM; (—) 2.0 μM; (—) 3.0 μM; (—) 4.0 μM; (—) 6.0 μM. **(b)** Stern-Volmer plot of insulin and $AuNPs^{piperine}$. **(c)** The plot of log ((F_0-F)/F) versus log [Q] for insulin binding with $AuNPs^{piperine}$. All the fluorescence measurements were carried out at room temperature in PBS buffer at pH 7.

5.1.5. Molecular interaction of native insulin with piperine:

To further understand the piperine-insulin interaction, molecular docking studies were performed to examine whether piperine has an inherent affinity for the aggregation prone residues of insulin. Using Discovery Studio (DS 4.0), blind docking studies were carried out (Dubey et al. 2015) and the obtained data are shown in Figure 5.8. The value of CDocker energy obtained for insulin-piperine interaction was found to be -19.4 kcal mol^{-1}. The structure of the insulin monomer-piperine complex, as shown in Figure 5.8, predicts interaction of the piperine molecule with the B-chain residues of insulin mediated by four hydrogen bonds and one pi-alkyl interaction (inset Table, Figure 5.8).

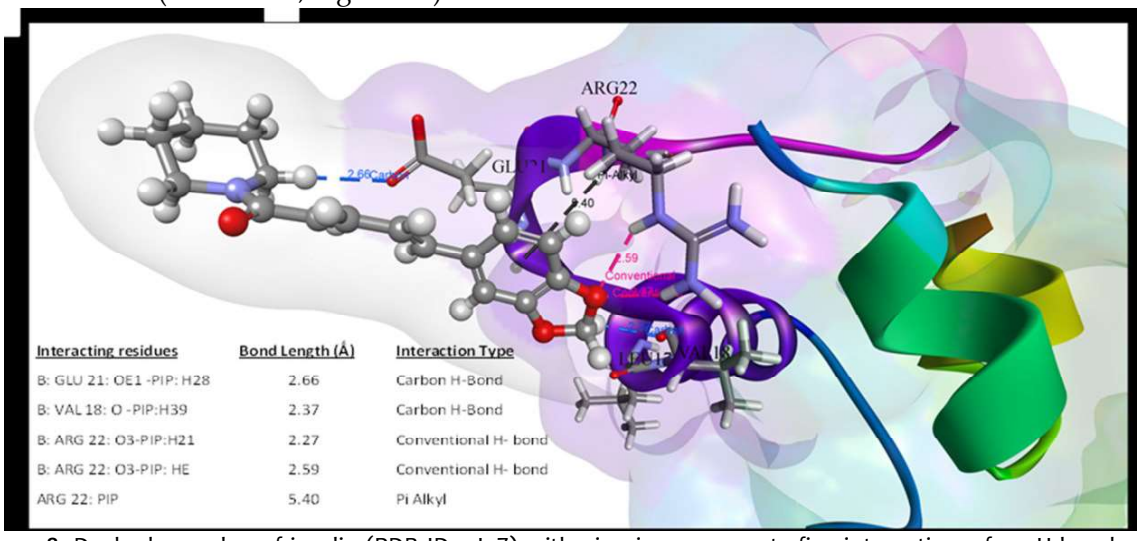

Figure 5.8: Docked complex of insulin (PDB ID: 4I5Z) with piperine represents five interactions: four H-bonds (GLU21:OE1-piperine:H28, VAL18: O-piperine:H39, ARG22:O3-piperine H21, ARG22:O3-piperine: HE) and one pi-alkyl interaction (ARG:22-piperine

It is well known that the B-chain segment "LVEALYL" plays a foundational role to begin the fibril formation of insulin(Ivanova et al. 2009). Notably, as evident from the docking data, piperine showed strong interactions with valine (V) and glutamic acid (E) residues of the aggregation prone segment (LVEALYL) of B-chain of insulin.

Prediction of aggregation propensity of insulin residues by AGGRECAN-3D tool (figure 5.9 and table 5.2) also suggests the binding of piperine with the aggregation prone residues of insulin. Hence, in this study, the binding of piperine with aggregation prone residues of insulin appears to be an important factor for the inhibition effect. Recent studies have already reported similar mechanism of inhibition of protein aggregation due to the binding of surface functionalized nanoparticles to the amyloidogenic core of the aggregating protein (Dubey et al. 2015)(Anand et al. 2016b).

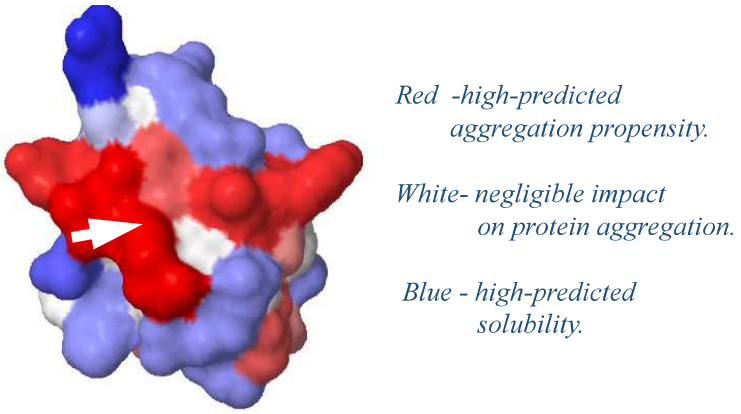

Figure 5.9. AGGRESCAN-3D analysis of INSULIN (PDB:4I5Z) structure obtained from AGGRESCAN online tool. The protein surface is colored according to A3D score in gradient from red (high-predicted aggregation propensity) to white (negligible impact on protein aggregation) to blue (high-predicted solubility). Arrow indicates the point of binding site of piperine as revealed by the docking studies (Figure 3b of the main text)

Table 5.2 AGGRESCAN 3D score for the aggregation prone amino acid residues in Insulin B chain (based on the A3Dscoring values).

Chain	Residue	Single letter	Aggrescan
1	F	B	1.9410
17	L	B	1.8385
25	F	B	1.8251
16	Y	B	1.4175
26	Y	B	0.8085
18	V	B	0.5360
24	F	B	0.5019
7	C	B	0.2271
27	T	B	0.0436
12	V	B	0.0382
2	V	B	0.0000
6	L	B	0.0000
11	L	B	0.0000
14	A	B	0.0000
15	L	B	0.0000
19	C	B	0.0000
30	A	B	-0.2528
23	G	B	-0.2914
28	P	B	-0.3828
8	G	B	-0.3946
9	S	B	-0.4690
20	G	B	-0.7954
5	H	B	-1.0113
10	H	B	-1.0288

5.1.6. Effect of piperine coated nanoparticle on collagen fibril assembly:

To address the issue of piperine's ability to interfere with the hydrophobic interactions between temperature induced partially folded species required to drive self-association of protein species, further experiments were carried out to know the effect of AuNPs^{piperine} on fibril formation of type I collagen extracted from rat tail tendon (RTT). Type I collagen, the most abundant form among collagens, is known to undergo a process of fibril formation at 37°C in PBS buffer (pH 7.4) (Perumal et al. 2015) and such process of self-assembly of collagen triple helical molecules is known to be driven by hydrophobic interactions (Cejas et al. 2008)(Kar et al. 2009). The turbidity data indicated that AuNPs^{piperine} inhibitors have the potential to supress the fibril formation of type I collagen (panel a of Figure 5.10). To generalize this inhibition effect of AuNPs^{piperine} on the fibril formation of type I collagen, its inhibition effect on the fibril formation of calf-skin collagen were tested and similar results were obtained (panel b, Figure 5.10). The morphologies of the collagen fibrils obtained from inhibited reactions (panel d and panel e, Figure 5.10) looked similar to the typical morphology observed for *in vitro* grown collagen fibrils(Savage et al. 1999).

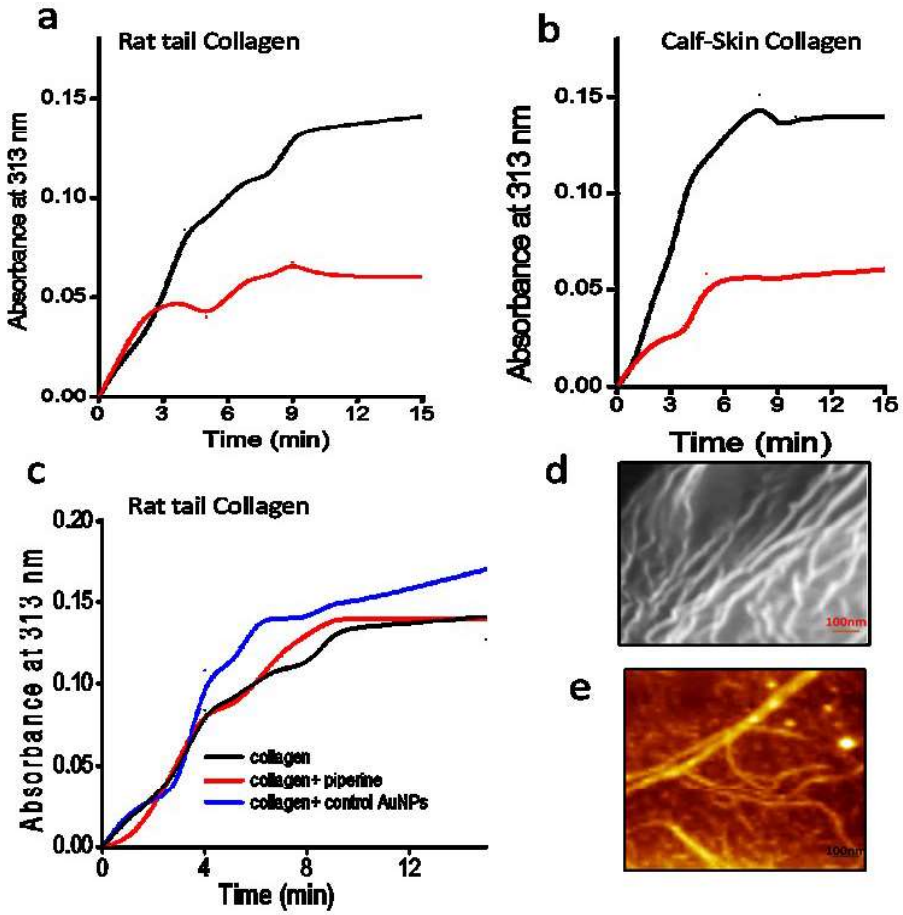

Figure 5.10: Effect of piperine coated gold nanoparticles on *in vitro* fibril formation process of type I collagen. (a) inhibition of rat tail tendon (RTT) collagen: (—) Collagen; (—) collagen + AuNPs^{piperine} (1:30). (b) inhibition of bovine calf-skin collagen: (—) collagen; (—) collagen + AuNPs^{piperine} (1:30). (c) Effect of isolated piperine and control uncoated gold nanoparticles at similar concentrations on fibril formation of RTT collagen, as labeled. (d) Scanning Electron microscopic image of mature fibrils of RTT collagen formed in the presence of AuNPs^{piperine}. (e) AFM images of mature fibrils of RTT collagen formed in the presence of AuNPs^{piperine}. All turbidity curves shown in this figure are the average representative of three acquisitions.

5.1.7 Biocompatibility studies of AuNPs^{piperine}.

After establishing the inhibition effect of the AuNPs^{piperine} against insulin aggregation, biocompatibility of these nanoparticle based inhibitors have been tested. The toxicity effect of these nanoparticles on the intact red blood cells was examined by following the established protocol for hemolysis assay (Mattson et al. 1997b). Data generated from the hemolysis assay experiments clearly indicate that no lysis of intact RBCs was observed in the presence of AuNPs^{piperine} (Figure 5.11 b, c). UV-vis spectra (Figure 5.11 b) did not show any indication of lysis of RBCs in the presence of AuNPs^{piperine} and this hemocompatibilty nature of the gold nanoparticles was further confirmed by SEM images (panel c of Figure 5.11 c.). Further, the effect of AuNPs^{piperine} on biological activity of proteins was also tested, considering lysozyme as a convenient model system. About ~ 25% enhancement of the catalytic efficiency of lysozyme was observed at pH 6.5 in the presence of AuNPs^{piperine} (Figure 5.11 a). Such an enhancement of lysozyme activity was not observed in the presence of isolated piperine at similar concentrations (data not shown), which further suggests the importance of surface functionalization of piperine for its bioactivity.

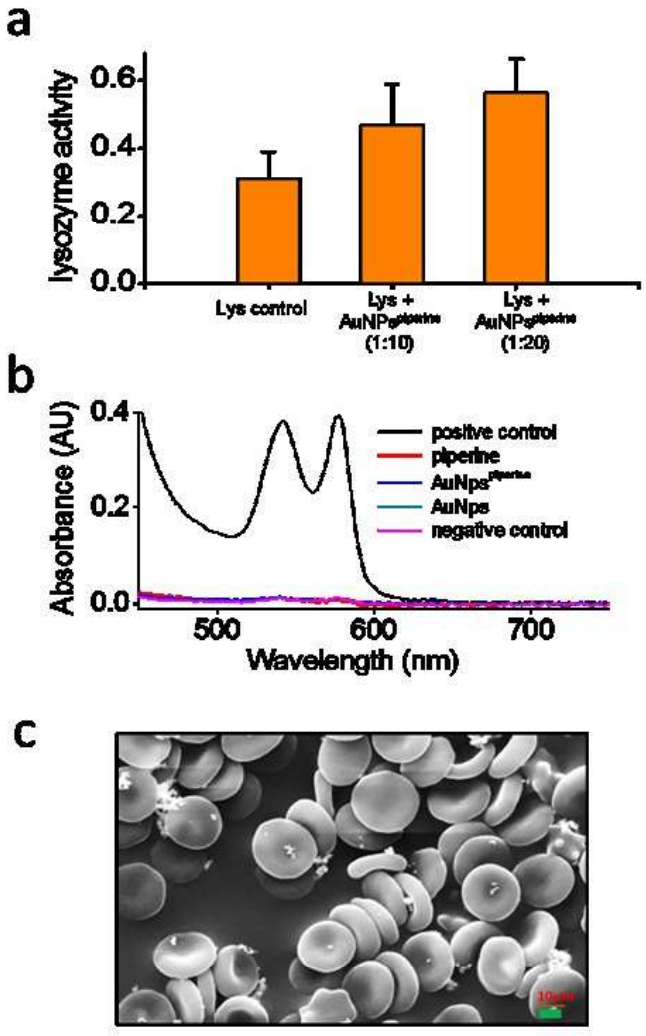

Figure 5.11 Biological compatibility of piperine coated gold nanoparticles. (a) Biological activity for lysozyme in presence of AuNPs^{piperine} as labelled. Activity assay was conducted at room temperature in PBS buffer at pH 6.5 (b) UV-visible spectra obtained from hemolysis assay: (—) RBCs in PBS buffer (positive control); (—) RBCs + 160 μM piperine; (—) RBCs + 160 μM AuNPs^{piperine} ;(—) RBCs + 160μM AuNPs; (—) RBCs in water (negative control). (c) SEM images (Scale bar 3μM) of intact RBC sample in the presence of AuNPs^{piperine}

5.2 DISCUSSION

Piperine (1-[5-(1,3-Benzodioxol-5-yl)-1-oxo-2,4-pentadienyl] piperidine(Schulz and Baranska 2007) has a unique structure comprising of piperidine moiety attached through a carbonyl amide linkage and a side chain consists of methylene dioxyphenyl ring. Piperine is known to strongly interact with different biomolecules including proteins and DNA (Chatani et al. 2014)(Zsila et al. 2005)(Haris et al. 2015)(Yeggoni et al. 2015). The C=O group, and both the oxygen atoms of the dioxalane ring of piperine are known to actively take part in H-bond interactions between piperine and DNA (Haris et al. 2015). Formation of H-bond interaction between valine residue of serum albumin and –O- (para) group of piperine molecule has been reported (Zsila et al. 2005). Further , binding of piperine with Androgenic Receptor (AR) protein has also been reported to involve two H-bond interactions: First interaction is between –O– (para) group of piperine with arginine residue (-NH_2 group), and the second one is between C=O of piperine with the valine residue (Yeggoni et al. 2015). Piperine is also known to directly interact with the arginine residue of human tear lipocalin protein via H-bonding interactions (Zsila et al. 2005). The obtained computational data reveal that valine and glutamic acid are the key interacting residues of insulin with piperine molecule (Figure 5.8). Both CD and Native PAGE data clearly suggest that the AuNPs^{piperine} inhibitors can retain the native conformation of insulin structure (panel b and panel e of Figure 5.5).

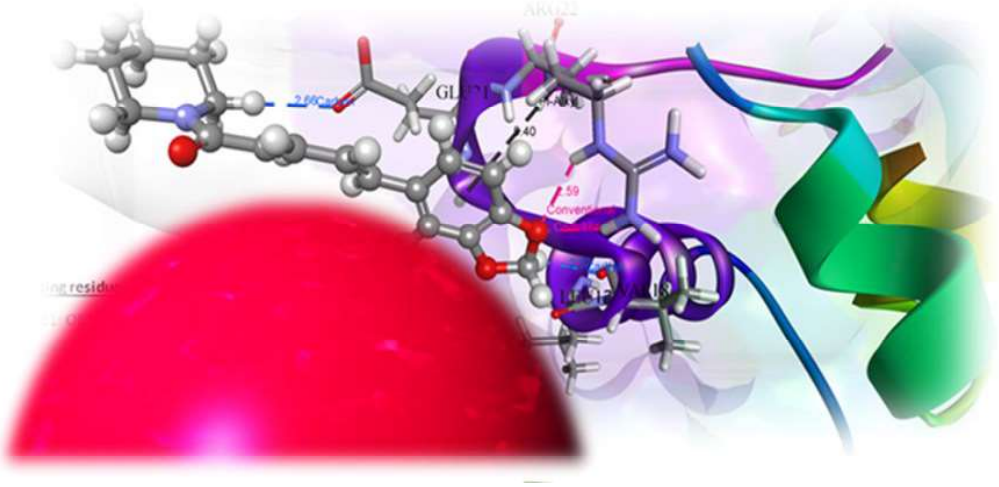

Figure 5.12. Schematic representation of insulin-AuNPs^{piperine} interaction.

It is predicted that the stabilization of the temperature induced partially folded insulin molecules could be one of the factors for the inhibition effect. It is possible that AuNPs^{piperine} inhibitors may interfere with the intermolecular hydrophobic interaction between partially folded aggregation prone species. Inhibition of amyloid fibril formation as well as collagen fibril formation suggests that piperine may have the potential to interfere with hydrophobic interactions necessary to initiate the self-assembly of protein molecules. It is important to notice that, isolated piperine and control gold nanoparticles did not show any such inhibition effect on type I collagen fibril formation (panel c, Figure S4) and on insulin fibril assembly, confirming the significance of surface functionalization of the inhibitor molecule. Conformational constraints and the hydrophobic nature of the inhibitor molecule are considered as two key factors to achieve the inhibition of amyloid fibril formation of proteins(Porat et al. 2006). We believe that the conjugation of piperine molecule with the gold nanoparticles may favour proper orientation of the C=O group, and both the oxygen atoms of its dioxalane moiety for an effective interaction with the respective functional groups of the amino acids located in the binding site of insulin. It also predicts that the size as well as the homogeneity of these

nanoparticles are critical to insulin-piperine interaction. On the issue of biocompatibility, it was observed that $AuNPs^{piperine}$ inhibitors are hemocompatible. These particles were also observed to enhance the activity of lysozyme. It is also important to notice that these nanoparticles are very stable at 70°C for a prolonged time (more than 4 weeks). This may be vital for the effective use of these inhibitors against temperature induced aggregation of protein species during their storage as therapeutic agents, particularly against insulin fibril assembly during its storage(Liza Nielsen et al. 2001) (Brange et al. 1992).

5.3. CONCLUSION

This study confirms that gold nanoparticles surface functionalized with piperine have the potential to prevent amyloid fibril formation of insulin under *in vitro* conditions. Surface functionalization of the gold nanoparticles with piperine seems to be critical for the inhibition effect because such strong inhibition of insulin fibril assembly was not observed in the presence of either isolated piperine or control gold nanoparticles. In addition to the antiamyloid activity, these piperine coated nanoparticles have the potential to prevent fibril formation of type I collagen. Stabilization of native structure of the protein, particularly binding of the inhibitior molecule to the aggregation prone residues of the insulin, appears to be one of the critical factors for the inhibition effect. The findings of this work on the ability of these hemocompatible and thermostable $AuNPs^{piperine}$ inhibitors to suppress insulin fibril assembly may be of great clinical significance.

...